

EMDS-6: Environmental Microorganism Image Dataset Sixth Version for Image Denoising, Segmentation, Feature Extraction, Classification and Detection Methods Evaluation

Peng Zhao^a, Chen Li^{a,*}, Md Mamanur Rahaman^{a,f}, Hao Xu^a, Pingli Ma^a, Hechen Yang^a, Hongzan Sun^d, Tao Jiang^b, Ning Xu^e and Marcin Grzegorzek^c

^a*Microscopic Image and Medical Image Analysis Group, MBIE College, Northeastern University, 110169, Shenyang, PR China*

^b*School of Control Engineering, Chengdu University of Information Technology, Chengdu 610225, China*

^c*University of Lübeck, Germany*

^d*Department of Radiology, Shengjing Hospital, China Medical University, Shenyang, 110122, China*

^e*School of Arts and Design, Liaoning Shihua University, Fushun 113001, China*

^f*School of Computer Science and Engineering, University of New South Wales, Sydney, Australia*

ARTICLE INFO

Keywords:

Environmental Microorganism
Image Denoising
Image Segmentation
Feature Extraction
Image Classification
Object Detection

ABSTRACT

Environmental microorganisms (EMs) are ubiquitous around us and have an important impact on the survival and development of human society. However, the high standards and strict requirements for the preparation of environmental microorganism (EM) data have led to the insufficient of existing related databases, not to mention the databases with GT images. This problem seriously affects the progress of related experiments. Therefore, This study develops the *Environmental Microorganism Dataset Sixth Version* (EMDS-6), which contains 21 types of EMs. Each type of EM contains 40 original and 40 GT images, in total 1680 EM images. In this study, in order to test the effectiveness of EMDS-6. We choose the classic algorithms of image processing methods such as image denoising, image segmentation and target detection. The experimental result shows that EMDS-6 can be used to evaluate the performance of image denoising, image segmentation, image feature extraction, image classification, and object detection methods. EMDS-6 is available at the URL: <https://doi.org/10.6084/m9.figshare.17125025.v1>.

1. Introduction

1.1. Environmental Microorganisms

Environmental Microorganisms (EMs) usually refer to tiny living that exists in nature and are invisible to the naked eye and can only be seen with the help of a microscope. Although they are small, they play an irreplaceable role in human survival and development [1]. Some beneficial bacteria can be used to produce fermented foods such as cheese and bread from a beneficial perspective. Meanwhile, Some beneficial EMs can degrade plastics, treat sulfur-containing waste gas in industrial, and improve the soil. From a harmful point of view, EMs cause food spoilage, reduce crop production and are also one of the chief culprits leading to the epidemic of infectious diseases. To make better use of the advantages of environmental microorganisms and prevent their harm, a large number of scientific researchers have joined the research of EMs. The image analysis of EM is the foundation of all this.

Generally, the size of the EMs are between 0.1 and 100 mm, which is challenging to be identified and found. Traditional microbial identification and analysis typically use the "morphological method," which requires a skilled operator to observe the EMs under a microscope [2]. Then, the results are presented according to the shape characteristics. This technique is very time-consuming and costly. There-

fore, using computer-assisted feature extraction and analysis of EM images can enable researchers to use their least professional knowledge with minimum time to make the most accurate decisions.

1.2. EM Image Analysis and Processing

Image analysis is a combination of mathematical models and image processing technology to analyze and extract certain intelligence information. Image processing refers to the use of computers to analyze images. Common processing includes image denoising, image segmentation and feature extraction. Image noise refers to various factors in the image that hinder people from accepting its information. Image noise is generally generated during image acquisition, transmission and compression [3]. The aim of image denoising is to recover the original image from the noisy image [4]. Image segmentation is a critical step of image processing to analyze an image. In the segmentation, we divide an image into several regions with unique properties and extract regions of interest [5]. Feature extraction is extracts valuable data or information from an image and obtains the "non-image" representation or description, such as values, vectors, and symbols [6]. Moreover, these characteristics can be distinguished from other types of objects. Using these features, we can classify images. Meanwhile, the features of an image are the basis of object detection. Object detection uses algorithms to generate object candidate frames, that is, object positions. Then, classify and regress the candidate frames.

*Corresponding author

 lichen201096@hotmail.com (C. Li)

1.3. The Contribution of Environmental Microorganism Image Dataset Sixth Version (EMDS-6):

Sample collections of the EMs are usually performed outdoors. When transporting or moving samples to the laboratory for observation, drastic changes in the environment and temperature affect the quality of EM samples. At the same time, if the researcher observes EMs under a traditional optical microscope, it is very prone to subjective errors due to continuous and long-term visual processing. Therefore, the collection of environmental microorganism image datasets is challenging [7]. Most of the existing environmental microorganism image datasets are not publicly available. This has a great impact on the progress of related scientific research. For this reason, we have created the *Environmental Microorganism Image Dataset Sixth Version* (EMDS-6) and made it publicly available to assist related scientific researchers. Compared with other environmental microorganism image datasets, EMDS-6 has many advantages. The database contains a variety of microorganisms and provides possibilities for multi-classification of EM images. In addition, each image of EMDS-6 has a corresponding ground truth (GT) image. GT images can be used for performance evaluation of image segmentation and target detection. However, the GT image production process is extremely complicated and consumes enormous time and human resources. Therefore, many environmental microorganism image dataset does not have GT images. However, our proposed dataset has GT images. In our experiments, EMDS-6 can provide robust data support in tasks such as denoising, image segmentation, feature extraction, image classification and object detection. Therefore, the main contribution of the EMDS-6 database is to provide data support for image analysis and image processing related research and promote the development of EMs related experiments and research.

2. EMDS-6 Database

There are 1680 images in the EMDS-6 database, including 21 classes of original EM images with 40 images per class, resulting in a total of 840 original images, and each original image is followed by a GT image for a total of 840. Table. 1 shows the details of the EMDS-6 database. Figure. 1 shows some examples of the original images and GT images in EMDS-6. EMDS-6 is freely published for non-commercial purpose at: <https://doi.org/10.6084/m9.figshare.17125025.v1>.

The collection process of EMDS-6 images starts from 2012 till 2020. The following people have made a significant contribution in producing the EMDS-6 dataset: Prof. Beihai Zhou and Dr Fangshu Ma from the University of Science and Technology Beijing, China; Prof. Dr.-Ing. Chen Li and M.E. HaoXu from Northeastern University, China; Prof. Yanling Zou from Heidelberg University, Germany. The GT images of the EMDS-6 dataset are produced by Prof. Dr.-Ing Chen Li, M.E. Bolin Lu, M.E. Xuemin Zhu and B.E. Huaqian Yuan from Northeastern University, China. The

GT image labelling rules are as follows: the area where the microorganism is located is marked as white as foreground, and the rest is marked as black as the background.

3. Evaluation of Denoising methods on the EMDS-6 Dataset

In digital image processing, the quality of an image to be recognized is often affected by external conditions, such as input equipment and the environment. The presence of noise largely affects image analysis and processing (e.g., image edge detection, image classification and segmentation). Therefore, image denoising is the key step of image preprocessing.

In this study, we have used four types of noise, Poisson noise, multiplicative noise, Gaussian noise and pretzel noise. By adjusting the mean, variance and density of different kinds of noise, a total of 13 specific noises are generated. They are multiplicative noise with a variance of 0.2 (marked as MN:0.2 in the table), multiplicative noise with a variance of 0.04 (MN:0.04), salt and pepper noise with a density of 0.01 (SPN:0.01), and salt and pepper noise with a density of 0.03. (SPN:0.03), pepper noise (PpN), salt noise (SN), Brightness Gaussian noise (BGN), Positional Gaussian noise (PGN), Gaussian noise with a variance of 0.01 and a mean of 0 (GN 0.01-0), Gaussian noise with a variance of 0.01 and a mean of 0.5 (GN 0.01-0.5), Gaussian noise with a variance of 0.03 and a mean of 0 (GN 0.03-0), Gaussian noise with a variance of 0.03 and a mean of 0.5 (GN 0.03-0.5), and Poisson noise (PN). There are 9 kinds of filters at the same time, namely Two-Dimensional Rank Order Filter (TROF), 3×3 Wiener Filter (WF (3 × 3)), 5×5 Wiener Filter (WF (5 × 5)), 3×3 Window Mean Filter (MF (3 × 3)), Mean Filter with 5×5 Window (MF (5 × 5)), Minimum Filtering (MinF), Maximum Filtering (MaxF), Geometric Mean Filtering (GMF), Arithmetic Mean Filtering (AMF). In the experiment, 13 kinds of noise are added to the EMDS-6 database image, and then 9 kinds of filters are used for filtering. The result of adding noise into the image and filtering is shown in Figure. 2. This paper uses two indicators, mean-variance and similarity, to evaluate filter performance.

The similarity evaluation index can be expressed as 1, where i represents the original image, i_1 represents the denoised image, N represents the number of pixels, and A represents the similarity between the denoised image and the original image. When the value of A is closer to 1, the similarity between the original image and the denoised image is higher, and the denoising effect is significant.

$$A = 1 - \frac{\sum_{i=1}^n |i_1 - i|}{N \times 255} \quad (1)$$

The variance evaluation index can be expressed as Eq. 2, where S denotes the mean-variance, $L_{(i,j)}$ represents the value corresponding to the coordinates of the original image

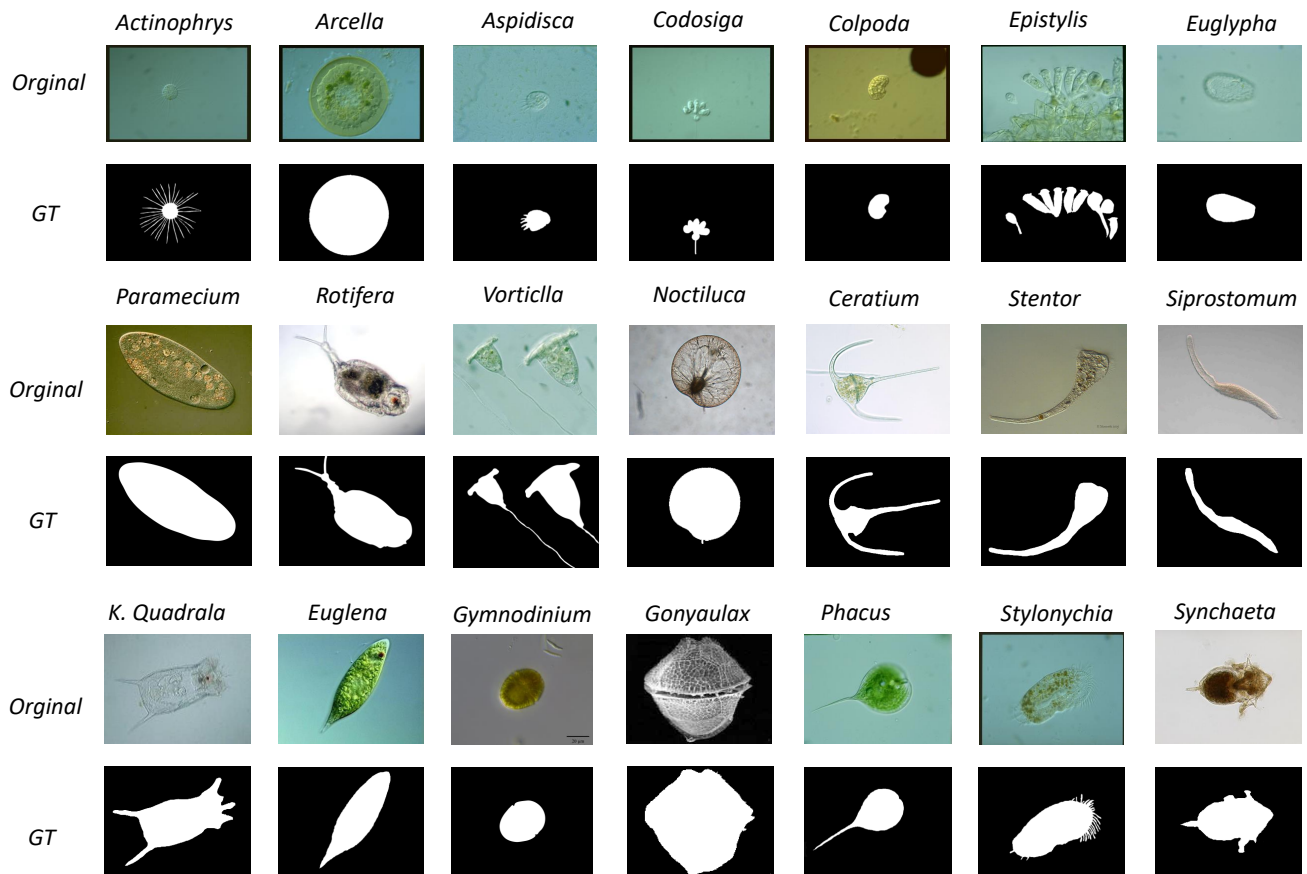


Figure 1: An example of EMDS-6, including original images and GT images.

Table 1

Basic information of EMDS-6 database, including Number of original images (NoOI), Number of GT images (NoGT).

Class	NoOI	NoGT	Class	NoOI	NoGT
Actinophrys	40	40	Ceratium	40	40
Arcella	40	40	Stentor	40	40
Aspidisca	40	40	Siprostomum	40	40
Codosiga	40	40	K. Quadrala	40	40
Colpoda	40	40	Euglena	40	40
Epistylis	40	40	Gymnodinium	40	40
Euglypha	40	40	Gonyaulax	40	40
Paramecium	40	40	Phacus	40	40
Rotifera	40	40	Stylonychia	40	40
Vorticilla	40	40	Synchaeta	-	-
Noctiluca	40	40	Total	840	840
Total	840	840			

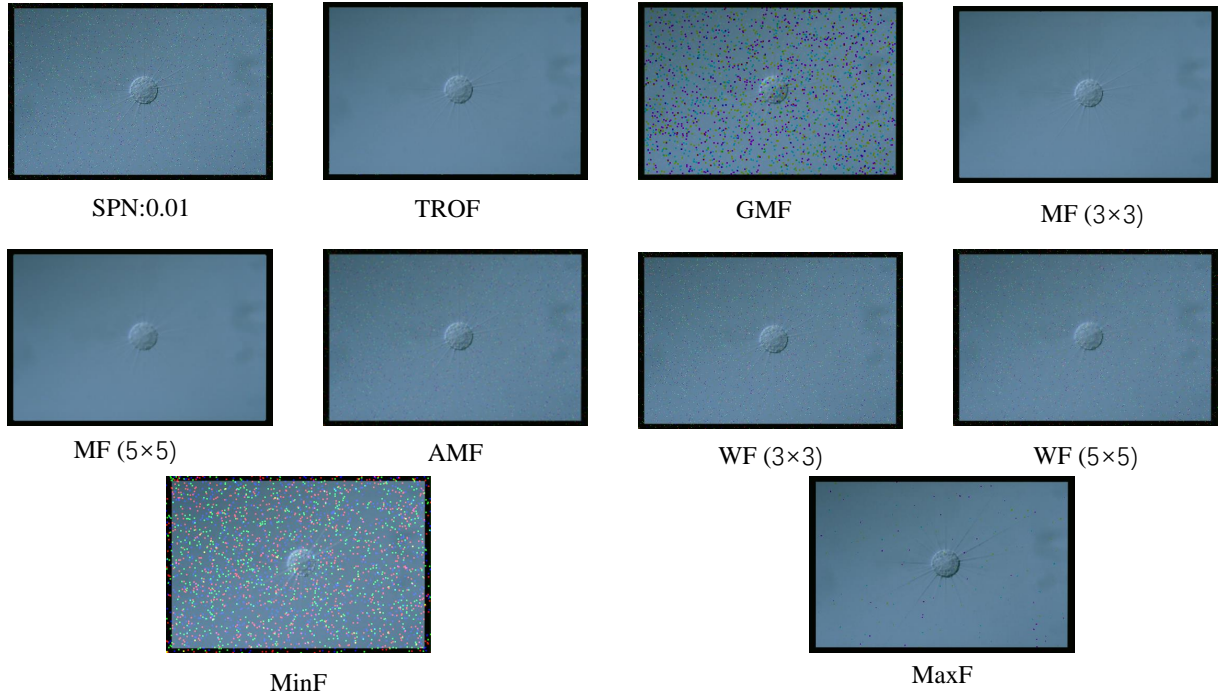


Figure 2: Examples of using different filters to filter salt and pepper noise.

(i, j) , and $B_{(i, j)}$ the value associated with the coordinates of the denoised image (i, j) . When the value of S is closer to 0, the higher the similarity between the original and denoised images, the better the denoising stability.

$$S = 1 - \frac{\sum_{i=1}^n (L_{(i, j)} - B_{(i, j)})^2}{\sum_{i=1}^n L_{(i, j)}^2} \quad (2)$$

We calculate the filtering effect of different filters for different noises. Their similarity evaluation indexes are shown in Table. 2. From Table. 2, it is easy to see that the GMF has a poor filtering effect for GN 0.01-0.5. The TROF and the MF have better filtering effects for MN:0.04.

In addition, the mean-variance is a common index to evaluate the stability of the denoising method. In this paper, the variance of the EMDS-6 denoised EM images and the original EM images are calculated as shown in Table. 3. As the noise density increases, the variance significantly increases among the denoised and the original images. For example, by increasing the SPN density from 0.01 to 0.03, the variance increases significantly under different filters. This indicates that the result after denoising is not very stable.

From the above experiments, EMDS-6 can test and evaluate the performance of image denoising methods well. Therefore, EMDS-6 can provide strong data support for EM image denoising research.

4. Evaluation of Segmentation methods on the EMDS-6 dataset

This paper designs the following experiment to prove that EMDS-6 can be used to test different image segmentation methods. Six classic segmentation methods are used in the experiment: k -means [8], Markov Random Field (MRF) [9], Otsu Thresholding [10], Region Growing (REG) [11], Region Split and Merge Algorithm (RSMA) [12] and Watershed Segmentation [13] and one deep learning-based segmentation method, Recurrent Residual CNN-based U-Net (U-Net) [14] are used in this experiment. While using U-Net for segmentation, 37.5% of the images are considered as the training set, 37.5% as the test set, and 25% as the validation set. We have calculated the Dice, Jaccard, and Recall evaluation metrics using segmented images and GT images.

Among the seven classical segmentation methods, k -means is based on clustering, which is a region-based technology. Watershed algorithm is based on geomorphological analysis such as mountains and basins to implement different object segmentation algorithms. MRF is an image segmentation algorithm based on statistics. Its main features are fewer model parameters and strong spatial constraints. Otsu Thresholding is an algorithm based on global binarization, which can realize adaptive thresholds. The REG segmentation algorithm starts from a certain pixel and gradually adds neighboring pixels according to certain criteria. When certain conditions are met, the regional growth is terminated, and object extraction is achieved. The RSMA is first to determine a split and merge criterion. When splitting to the

Table 2

Similarity comparison between denoised image and original image. Types of noise (ToN), Denoising method (DM). (In [%].).

ToN / DM	TROF	MF: (3×3)	MF: (5×5)	WF: (3×3)	WF: (5×5)	MaxF	MinF	GMF	AMF
PN	98.36	98.24	98.00	98.32	98.15	91.97	99.73	99.21	98.11
MN:0.2	99.02	90.29	89.45	91.98	91.08	71.15	99.02	98.89	90.65
MN:0.04	99.51	99.51	99.51	95.57	95.06	82.35	99.51	98.78	94.92
GN 0.01-0	96.79	96.45	96.13	96.75	96.40	85.01	99.44	98.93	96.28
GN 0.01-0.5	98.60	98.52	98.35	98.97	98.81	96.32	99.67	64.35	98.73
GN 0.03-0	94.64	93.99	93.56	94.71	94.71	76.46	99.05	98.74	93.82
GN 0.03-0.5	97.11	96.95	96.66	98.09	97.79	94.04	99.24	66.15	97.54
SPN:0.01	99.28	99.38	99.14	99.60	99.37	95.66	99.71	99.44	99.16
SPN:0.03	98.71	98.57	98.57	99.29	98.87	92.28	99.24	99.26	98.80
PpN	98.45	98.53	98.30	99.46	99.02	96.30	99.04	99.61	98.61
BGN	97.93	97.74	97.74	97.91	97.69	90.00	99.66	99.16	97.60
PGN	96.97	96.63	96.33	97.16	96.85	85.82	99.47	98.98	96.47
SN	97.90	97.97	97.75	99.27	98.63	99.27	98.63	99.64	98.15

Table 3

Comparison of variance between denoised image and original image. (In [%].).

ToN / DM	TROF	MF: (3×3)	MF: (5×5)	WF: (3×3)	WF: (5×5)	MaxF	MinF	GMF	AMF
PN	1.49	0.77	1.05	0.52	0.66	3.68	2.99	0.41	0.88
MN,v: 0.2	32.49	14.94	15.65	9.33	11.36	39.22	32.49	4.32	13.35
MN,v: 0.04	10.89	10.89	10.89	2.99	3.71	14.41	10.89	0.98	4.28
GN,m: 0,v: 0.01	3.81	3.06	3.44	2.06	2.62	11.68	7.36	1.16	3.00
GN,m: 0.5,v: 0.01	0.89	0.36	0.41	0.21	0.28	0.99	1.74	61.93	0.43
GN,m: 0,v: 0.03	8.60	7.78	8.34	5.04	5.04	27.23	16.55	4.24	7.33
GN,m: 0.5,v: 0.03	1.60	1.08	1.18	0.55	0.73	2.39	3.06	56.17	1.05
SPN,d: 0.01	1.92	1.21	1.46	0.10	0.30	6.37	2.90	4.73	1.25
SPN,d: 0.03	3.84	3.39	3.39	0.33	1.09	14.64	5.18	13.02	3.15
PpN	2.88	2.18	2.44	0.17	0.72	3.72	4.48	16.84	2.09
BGN	2.35	1.63	1.94	1.09	1.38	6.67	4.57	0.84	1.66
PGN	3.79	3.04	3.42	1.67	2.13	11.56	7.33	1.23	2.98
SN	3.86	3.17	3.44	0.31	1.35	4.82	6.25	5.58	2.94

point of no further division, the areas with similar characteristics are integrated. Figure. 3 shows a sample of the results of different segmentation methods on EMDS-6.

Among the three evaluation metrics, the Dice coefficient is pixel-level, and the Dice coefficient takes a range of 0-1. The more close to 1, the better the structure of the model. The Jaccard coefficient is often used to compare the similarity between two samples. When the Jaccard coefficient

is larger, the similarity between the samples is higher. The recall is a measure of coverage, mainly for the accuracy of positive sample prediction. The computational expressions of Dice, Jaccard, and Recall are shown in Table. 4.

The evaluation results of the above image segmentation methods are shown in Table. 5. The REG and RSMA have poor segmentation performance, and their Dice, Jaccard, and Recall indexes are much lower than other segmentation meth-

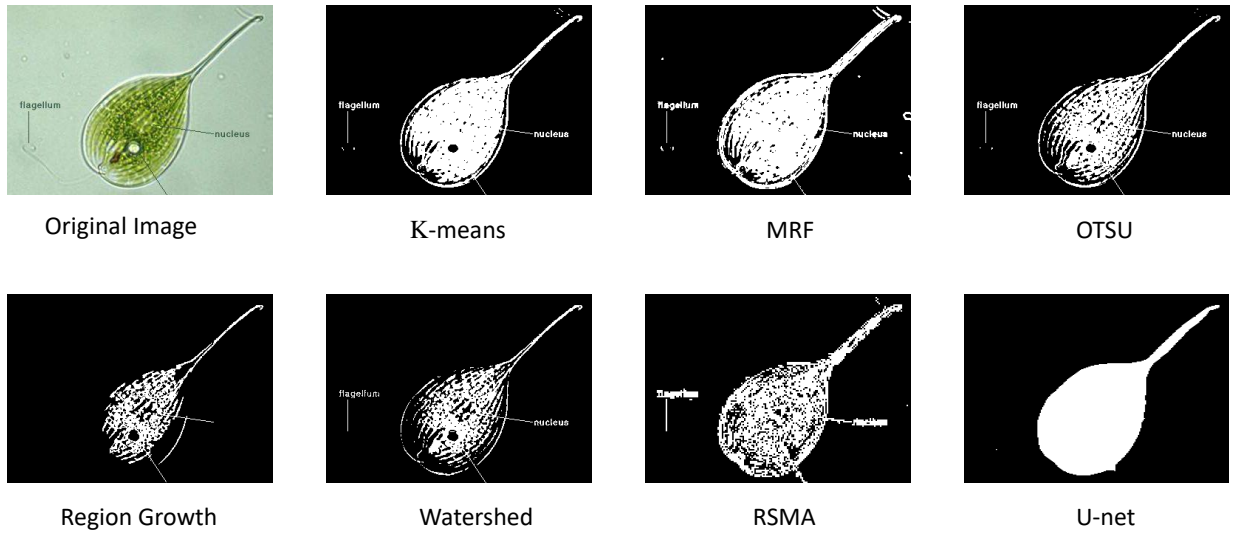


Figure 3: Output of results of different segmentation methods.

Table 4

Evaluation metrics of segmentation method. TP (True Positive), FN (False Negative), V_{pred} (Represents the foreground predicted by the model), V_{gt} (represents the foreground in a GT image.).

Indicators	Formula
Dice	$\frac{2 \times V_{pred} \cap V_{gt} }{ V_{pred} + V_{gt} }$
Jaccard	$\frac{ V_{pred} \cap V_{gt} }{ V_{pred} \cup V_{gt} }$
Recall	$\frac{TP}{TP + FN}$

ods. However, the deep learning-based, U-net, has provided superior performance. By comparing these image segmentation methods, it can be concluded that EMDS-6 can provide strong data support for testing and assessing image segmentation methods.

5. Image Feature Extraction Evaluation Based on EMDS-6

This paper uses ten methods for feature extraction, including two-colour features, One is HSV (Hue, Saturation and Value) feature [15], and the other is RGB (Red, Green and Blue) colour histogram feature [16]. The three texture features include the Local Binary Pattern (LBP) [17], the Histogram of Oriented Gradient (HOG) [18] and the Gray-level Cooccurrence Matrix (GLCM) [19] formed by the recurrence of pixel gray Matrix. The four geometric features (Geo) [20] include perimeter, area, long-axis and short-axis and seven invariant moment features (Hu) [21]. The perimeter, area, long-axis and short-axis features are extracted from

Table 5

Evaluation of Feature Extraction methods using EMDS-6 dataset. (In [%].).

Method/Index	Dice	Jaccard	Recal
k-means	47.78	31.38	32.11
MRF	56.23	44.43	69.94
Otsu	45.23	33.82	40.60
REG	29.72	21.17	26.94
RSMA	37.35	26.38	30.18
Watershed	44.21	32.44	40.75
U-Net	88.35	81.09	89.67

the GT image, while the rest are extracted from the original image. Finally, we use a support vector machine (SVM) to classify the extracted features. The classifier parameters are shown in Table. 6.

In this paper, we use the SVM to classify different features. The classification results are shown in Table. 7. In Table. 7, the SVM classifies different features with very different results. The Hu features performed poorly, while the Geo features performed the best. By comparing these classification results, we can conclude that EMDS-6 can be used to evaluate image features.

6. Evaluation of Classification methods using EMDS-6 dataset

This paper designed the following two experiments to test the EMDS-6 dataset. Experiment 1: use traditional machine learning methods to classify images. Since we have seen that the Geo feature provides good classification per-

Table 6

Parameter setting of EMDS-6 feature classification using SVM. C (penalty coefficient), decision function shape (DFS), The error value of stopping training (tol), Geometric features (Geo).

Feature	Kernel	C	DFS	tol	Max iter
LBP	rbf	50000	ovr	1e-3	-1
GLCM	rbf	10000	ovr	1e-3	-1
HOG	rbf	1000	ovr	1e-3	-1
HSV	rbf	100	ovr	1e-3	-1
Geo	rbf	2000000	ovr	1e-3	-1
Hu	rbf	100000	ovr	1e-3	-1
RGB	rbf	20	ovr	1e-3	-1

Table 7

Different results obtained by applying different features in the EMDS-6 classification experiments using SVM. Feature type (FT), Accuracy (Acc). (In [%].).

FT	LBP	GLCM	HOG
Acc	32.38	10.24	22.98
HSV	Geo	Hu	RGB
29.52	50.0	7.86	28.81

formance in section 5, this chapter uses Geo features to verify the classifier's performance. Moreover, traditional classifiers used for testing includes, three k -Nearest Neighbor (k NN) classifiers ($k=1, 5, 10$) [22], three Random Forests (RF) (tree=10, 20, 30) [23] and four SVMs (kernel function=rbf, polynomial, sigmoid, linear) [24]. In terms of data distribution, we have selected 50% of images from the EMDS-6 dataset as the training set, and the rest are considered as the test set. Finally, the evaluation metrics are used to evaluate the performance of each classifier, as shown in Table. 8.

It can be seen from Table. 8 that the RF classifier has the best classification effect. However, the performance of the SVM classifier using the sigmoid kernel function is relatively poor. In addition, there is a big difference in Accuracy between other classical classifiers. By comparing these traditional classification methods, we can conclude that the EMDS-6 dataset can be used to test and evaluate the performance of traditional image classification methods.

In experiment 2, we have used deep learning-based methods to classify images. 37.5% of the EMDS-6 dataset is considered as a training set, 25% as the validation set, and 37.5% as the test set.

In this experiment, 21 classifiers are used to evaluate the performance, including, ResNet-18, 34, 50, 101 [25], VGG-11, 13, 16, 19 [26], DenseNet-121, 169 [27], Inception-V3 [28], Xception [29], AlexNet [30], GoogleNet [31], MobileNetV2 [32], ShuffeleNetV2 [33], Inception-ResNet -V1 [34],

and a series of VTs, such as ViT [35], BotNet [36], DeiT [37], T2T-ViT [38]. In addition, this comparative experiment is carried out on a local computer. The specific hardware operating environment is shown in Table. 10. The computer software operating environment is as follows: Win10 Professional operating system, Python 3.6 and Pytorch 1.7.1. At the same time, the code runs in the integrated development environment Pycharm 2020 Community Edition. The hyper-parameters uniformly set for each model are shown in Table. 11. In order to scientifically evaluate the classification performance of the deep learning model, we have calculated the precision, recall, accuracy, F1-score, the size of the model parameters, and the training and validation time as shown in Table. 9.

According to Table. 9, the Xception network performs the best on the EMDS-6 dataset. The training time of the ViT model is the least. The classification performance of the ShuffleNet-V2 network is average, but the number of parameters is the least. Therefore, ShuffleNet-V2 is more suitable for occasions where high classification performance is not required and limited storage space. Therefore, we can conclude that the EMDS-6 dataset can be used to test and evaluate the performance of the classification methods.

7. Evaluation of Object Detection Methods Using EMDS-6 Dataset

Faster RCNN [39] and Mask RCNN [40] is used to test the feasibility of the EMDS-6 dataset for object detection. Faster RCNN provide excellent performance in many areas of object detection. Good results have been achieved in many areas of object detection. The Mask RCNN is optimized on the original framework of Faster RCNN. By using a better skeleton (ResNet combined with FPN) and the AlignPooling algorithm, Mask RCNN achieves better detection results than Faster RCNN.

In this experiment, we used 25% of the EMDS-6 data as training, 25% is for validation, and the rest is for testing. In addition, Average Precision (AP) and Mean Average Precision (mAP) is calculated to evaluate the test results. AP is a model evaluation index widely used in object detection. The higher the AP, the fewer detection errors. AP calculation method is shown in Eq 3 and Eq 4.

$$AP = \sum_{n=1}^N (r_{n+1} - r_n) P_{\text{interp}}(r_{n+1}) \quad (3)$$

$$P_{\text{interp}}(r_{n+1}) = \max_{\hat{r}=r_{n+1}} = P(\hat{r}) \quad (4)$$

Among them, r_n represents the value of the nth recall, and $p(\hat{r})$ represents the value of precision when the recall is \hat{r} .

We can see from Table. 12 that Faster RCNN and Mask RCNN have very different object detection effects based on their AP value. Among them, the Faster RCNN model has

Table 8

Classification results of Geo features by different classifiers. (In [%].).

Classifier type	SVM: linear	SVM: polynomial	SVM: RBF	SVM: sigmoid	RF,nT: 30
Accuracy	51.67	27.86	28.81	14.29	98.33
k NN,k: 1	k NN,k: 5	k NN,k: 10	RF,nT: 10	RF,nT: 20	—
23.1	17.86	17.38	96.19	97.86	—

Table 9

Classification results of different deep learning models. Accuracy (Acc), Params Size (PS)

Model	Precision (%)	Recall (%)	F1_score (%)	Acc (%)	PS (MB)	Time (s)
Xception	45.71%	52.48%	44.95%	45.71%	79.8	996
ResNet34	42.86%	45.33%	42.31%	42.86%	81.3	780
Googlenet	41.90%	42.83%	40.49%	41.91%	21.6	772
Densenet121	40.95%	43.61%	40.09%	40.95%	27.1	922
Densenet169	40.95%	43.62%	39.89%	40.95%	48.7	988
ResNet18	40.95%	45.55%	41.05%	40.95%	42.7	739
Inception-V3	40.00%	45.01%	39.70%	40.00%	83.5	892
Mobilenet-V2	39.52%	39.57%	37.01%	39.52%	8.82	767
InceptionResnetV1	39.05%	41.54%	37.96%	39.05%	30.9	800
Deit	39.05%	39.37%	37.70%	39.05%	21.1	817.27
ResNet50	38.57%	43.84%	38.02%	38.57%	90.1	885
ViT	37.14%	41.02%	35.95%	37.14%	31.2	715
ResNet101	34.76%	36.52%	32.99%	34.76%	162	1021
T2T-ViT	34.29%	38.17%	34.54%	34.28%	15.5	825.3
ShuffleNet-V2	33.81%	33.90%	31.68%	33.81%	1.52	713
AlexNet	31.90%	32.53%	29.32%	31.91%	217	712
VGG11	31.43%	41.20%	29.97%	31.43%	491	864
BotNet	30.48%	32.61%	30.06%	30.48%	72.2	894
VGG13	20.95%	19.23%	18.37%	20.95%	492	957
VGG16	9.05%	1.31%	2.10%	9.05%	512	990
VGG19	4.76%	0.23%	0.44%	4.76%	532	1036

Table 10

Computer hardware configuration.

Hardware	Product Number
SSD	HP SSD S750 256GB
CPU	Intel Core i7-10700
GPU	NVIDIA Quadro RTX 4000

the best effect on Actinophrys object detection. The Mask RCNN model has the best effect on Arcella object detection.

Table 11

Deep learning model parameters.

Parameter	Parameter
Batch Size , 32	Epoch , 100
Learning , 0.002	Optimizer , Adam

Based on the mAP value, it is seen that Faster RCNN is better than Mask RCNN for object detection. The result of object detection is shown in Figure 4. Most of the EMs in the pic-

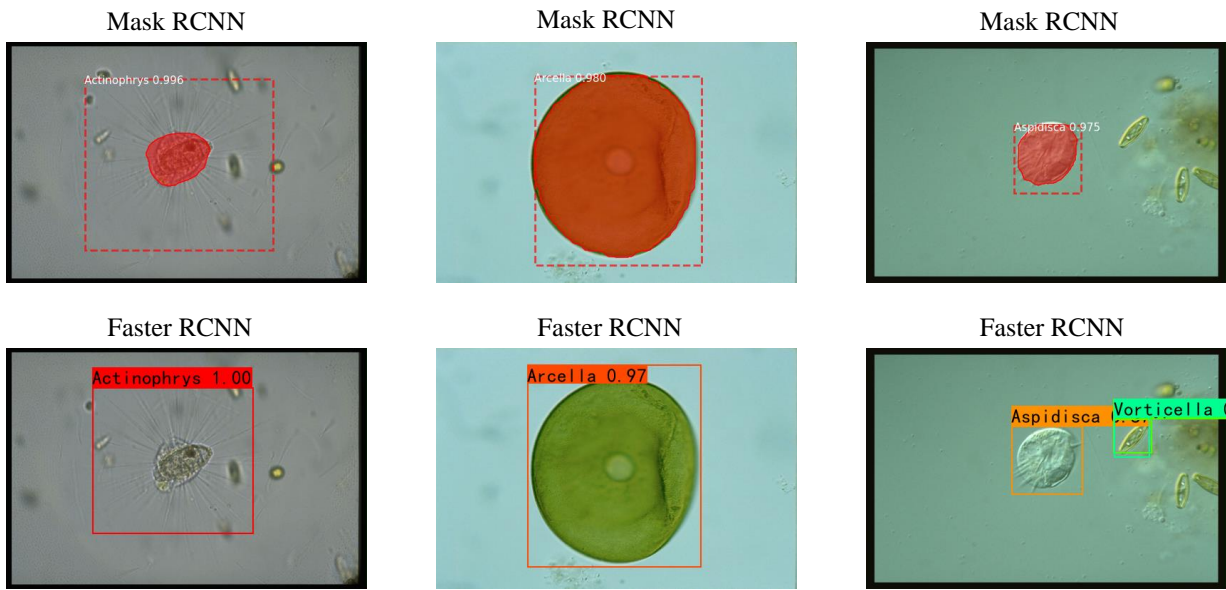


Figure 4: Faster RCNN and Mask RCNN object detection results.

Table 12
AP and mAP based on EMDS-6 object detection of different types of EMs.

Model\Sample (AP)	Actinophrys	Arcella	Aspidisca	Codosiga	Colpoda	Epistylis	Euglypha	Paramecium
Faster RCNN	0.95	0.75	0.39	0.13	0.52	0.24	0.68	0.70
Mask RCNN	0.7	0.85	0.4	0.175	0.35	0.525	0.25	0.7
Model\Sample	Rotifera	Vorticella	Noctiluca	Ceratium	Stentor	Siprostomum	K.Quadrata	Euglena
Faster RCNN	0.69	0.30	0.56	0.61	0.47	0.60	0.22	0.37
Mask RCNN	0.4	0.15	0.9	0.7	0.65	0.7	0.45	0.25
Model\Sample	Gymnodinium	Gonyaulax	Phacus	Stylongchia	Synchaeta	mAP	–	–
Faster RCNN	0.53	0.25	0.43	0.42	0.61	0.4962	–	–
Mask RCNN	0.6	0.275	0.5	0.675	0.475	0.5083	–	–

ture can be accurately marked. Therefore it is demonstrated that the EMDS-6 dataset can be effectively applied to image object detection.

8. Conclusion and Future Work

This paper develops an environmental microorganism image datasets, namely EMDS-6. EMDS-6 contains 21 types of EMs and a total of 1680 images. Including 840 original images and 840 GT images of the same size. Each type of EMs has 40 original images and 40 GT images. In the test, 13 kinds of noises such as multiplicative noise and salt and pepper noise are used, and nine kinds of filters such as Wiener filter and geometric mean filter are used to test the denoising effect of various noises. The experimental results

prove that EMDS-6 has the function of testing the filter denoising effect. In addition, this paper uses 6 traditional segmentation algorithms such as *k*-means and MRF and one deep learning algorithm to compare the performance of the segmentation algorithm. The experimental results prove that EMDS-6 can effectively test the image segmentation effect. At the same time, in the image feature extraction and evaluation experiment, this article uses 10 features such as HSV and RGB extracted from EMDS-6. Meanwhile, the SVM classifier is used to test the features. It is found that the classification results of different features are significantly different, and EMDS-6 has the function of testing the pros and cons of features. In terms of image classification, this paper designs two experiments. The first experiment uses three

classic machine learning methods to test the classification performance. The second experiment uses 21 deep learning models. At the same time, indicators such as accuracy and training time are calculated to verify the performance of the model from multiple dimensions. The results show that EMDS-6 can effectively test the image classification performance. In terms of object detection, this paper tests Faster RCNN and Mask RCNN, respectively. Most of the EMs in the experiment can be accurately marked. Therefore, EMDS-6 can be effectively applied to image object detection.

In the future, we will further expand the number of EM images of EMDS-6. At the same time, we will try to apply EMDS-6 to more computer vision processing fields to further promote microbial research development.

Acknowledgments

This work is supported by the “National Natural Science Foundation of China” (No.61806047) and the “Fundamental Research Funds for the Central Universities” (No. N2019003). We thank Miss Zixian Li and Mr. Guoxian Li for their important discussion.

Declaration of Competing Interest

The authors declare that they have no conflict of interest in this paper.

References

- [1] Michael T Madigan, John M Martinko, Jack Parker, et al. *Brock biology of microorganisms*, volume 11. Prentice hall Upper Saddle River, NJ, 1997.
- [2] Eugene L Madsen. *Environmental microbiology: from genomes to biogeochemistry*. John Wiley & Sons, 2015.
- [3] Ioannis Pitas. *Digital image processing algorithms and applications*. John Wiley & Sons, 2000.
- [4] Antoni Buades, Bartomeu Coll, and Jean-Michel Morel. A review of image denoising algorithms, with a new one. *Multiscale modeling & simulation*, 4(2):490–530, 2005.
- [5] Shervin Minaee, Yuri Y Boykov, Fatih Porikli, Antonio J Plaza, Nasser Kehtarnavaz, and Demetri Terzopoulos. Image segmentation using deep learning: A survey. *IEEE Transactions on Pattern Analysis and Machine Intelligence*, 2021.
- [6] Rizgar Zebari, Adnan Abdulazeez, Diyar Zeebaree, Dilovan Zebari, and Jwan Saeed. A comprehensive review of dimensionality reduction techniques for feature selection and feature extraction. *Journal of Applied Science and Technology Trends*, 1(2):56–70, 2020.
- [7] Sergey Kosov, Kimiaki Shirahama, Chen Li, and Marcin Grzegorzek. Environmental microorganism classification using conditional random fields and deep convolutional neural networks. *Pattern recognition*, 77:248–261, 2018.
- [8] SM Ajil Burney and Humera Tariq. K-means cluster analysis for image segmentation. *International Journal of Computer Applications*, 96(4), 2014.
- [9] Zoltan Kato, Josiane Zerubia, et al. *Markov random fields in image segmentation*. Now, 2012.
- [10] Nobuyuki Otsu. A threshold selection method from gray-level histograms. *IEEE transactions on systems, man, and cybernetics*, 9(1):62–66, 1979.
- [11] Rolf Adams and Leanne Bischof. Seeded region growing. *IEEE Transactions on pattern analysis and machine intelligence*, 16(6):641–647, 1994.
- [12] Shiu-Yung Chen, Wei-Chung Lin, and Chin-Tu Chen. Split-and-merge image segmentation based on localized feature analysis and statistical tests. *CVGIP: Graphical Models and Image Processing*, 53(5):457–475, 1991.
- [13] Ilya Levner and Hong Zhang. Classification-driven watershed segmentation. *IEEE Transactions on Image Processing*, 16(5):1437–1445, 2007.
- [14] Md Zahangir Alom, Chris Yakopcic, Mahmudul Hasan, Tarek M Taha, and Vijayan K Asari. Recurrent residual u-net for medical image segmentation. *Journal of Medical Imaging*, 6(1):014006, 2019.
- [15] Chen Junhua and Lei Jing. Research on color image classification based on hsv color space. In *2012 Second International Conference on Instrumentation, Measurement, Computer, Communication and Control*, pages 944–947. IEEE, 2012.
- [16] JC Kavitha and A Suruliandi. Texture and color feature extraction for classification of melanoma using svm. In *2016 International conference on computing technologies and intelligent data engineering (ICCTIDE'16)*, pages 1–6. IEEE, 2016.
- [17] Timo Ojala, Matti Pietikainen, and Topi Maenpaa. Multiresolution gray-scale and rotation invariant texture classification with local binary patterns. *IEEE Transactions on pattern analysis and machine intelligence*, 24(7):971–987, 2002.
- [18] Navneet Dalal and Bill Triggs. Histograms of oriented gradients for human detection. In *2005 IEEE computer society conference on computer vision and pattern recognition (CVPR'05)*, volume 1, pages 886–893. Ieee, 2005.
- [19] Hou Qunqun, Wang Fei, and Yan Li. Extraction of color image texture feature based on gray-level co-occurrence matrix. *Remote Sensing for Land & Resources*, 25(4):26–32, 2013.
- [20] KBRK Ramesha, KB Raja, KR Venugopal, and LM Patnaik. Feature extraction based face recognition, gender and age classification. *International Journal on Computer Science and Engineering*, 2:14–23, 2010.
- [21] Ming-Kuei Hu. Visual pattern recognition by moment invariants. *IRE transactions on information theory*, 8(2):179–187, 1962.
- [22] Teminda Abeywickrama, Muhammad Aamir Cheema, and David Taniar. K-nearest neighbors on road networks: a journey in experimentation and in-memory implementation. *arXiv preprint arXiv:1601.01549*, 2016.
- [23] Tin Kam Ho. Random decision forests. In *Proceedings of 3rd international conference on document analysis and recognition*, volume 1, pages 278–282. IEEE, 1995.
- [24] Mayank Arya Chandra and SS Bedi. Survey on svm and their application in image classification. *International Journal of Information Technology*, pages 1–11, 2018.
- [25] Kaiming He, Xiangyu Zhang, Shaoqing Ren, and Jian Sun. Deep residual learning for image recognition. In *Proceedings of the IEEE conference on computer vision and pattern recognition*, pages 770–778, 2016.
- [26] Karen Simonyan and Andrew Zisserman. Very deep convolutional networks for large-scale image recognition. *arXiv preprint arXiv:1409.1556*, 2014.
- [27] Gao Huang, Zhuang Liu, Laurens Van Der Maaten, and Kilian Q Weinberger. Densely connected convolutional networks. In *Proceedings of the IEEE conference on computer vision and pattern recognition*, pages 4700–4708, 2017.
- [28] Christian Szegedy, Vincent Vanhoucke, Sergey Ioffe, Jon Shlens, and Zbigniew Wojna. Rethinking the inception architecture for computer vision. In *Proceedings of the IEEE conference on computer vision and pattern recognition*, pages 2818–2826, 2016.
- [29] François Chollet. Xception: Deep learning with depthwise separable convolutions. In *Proceedings of the IEEE conference on computer vision and pattern recognition*, pages 1251–1258, 2017.
- [30] Alex Krizhevsky, Ilya Sutskever, and Geoffrey E Hinton. Imagenet classification with deep convolutional neural networks. *Advances in neural information processing systems*, 25:1097–1105, 2012.
- [31] Christian Szegedy, Wei Liu, Yangqing Jia, Pierre Sermanet, Scott Reed, Dragomir Anguelov, Dumitru Erhan, Vincent Vanhoucke, and

Andrew Rabinovich. Going deeper with convolutions. In *Proceedings of the IEEE conference on computer vision and pattern recognition*, pages 1–9, 2015.

[32] Mark Sandler, Andrew Howard, Menglong Zhu, Andrey Zhmoginov, and Liang-Chieh Chen. Mobilenetv2: Inverted residuals and linear bottlenecks. In *Proceedings of the IEEE conference on computer vision and pattern recognition*, pages 4510–4520, 2018.

[33] Ningning Ma, Xiangyu Zhang, Hai-Tao Zheng, and Jian Sun. Shufflenet v2: Practical guidelines for efficient cnn architecture design. In *Proceedings of the European conference on computer vision (ECCV)*, pages 116–131, 2018.

[34] Christian Szegedy, Sergey Ioffe, Vincent Vanhoucke, and Alexander Alemi. Inception-v4, inception-resnet and the impact of residual connections on learning. In *Proceedings of the AAAI Conference on Artificial Intelligence*, volume 31, 2017.

[35] Alexey Dosovitskiy, Lucas Beyer, Alexander Kolesnikov, Dirk Weissenborn, Xiaohua Zhai, Thomas Unterthiner, Mostafa Dehghani, Matthias Minderer, Georg Heigold, Sylvain Gelly, et al. An image is worth 16x16 words: Transformers for image recognition at scale. *arXiv preprint arXiv:2010.11929*, 2020.

[36] Aravind Srinivas, Tsung-Yi Lin, Niki Parmar, Jonathon Shlens, Pieter Abbeel, and Ashish Vaswani. Bottleneck transformers for visual recognition. *arXiv preprint arXiv:2101.11605*, 2021.

[37] Hugo Touvron, Matthieu Cord, Matthijs Douze, Francisco Massa, Alexandre Sablayrolles, and Hervé Jégou. Training data-efficient image transformers & distillation through attention. *arXiv preprint arXiv:2012.12877*, 2020.

[38] Li Yuan, Yunpeng Chen, Tao Wang, Weihao Yu, Yujun Shi, Francis EH Tay, Jiashi Feng, and Shuicheng Yan. Tokens-to-token vit: Training vision transformers from scratch on imagenet. *arXiv preprint arXiv:2101.11986*, 2021.

[39] Shaoqing Ren, Kaiming He, Ross Girshick, and Jian Sun. Faster r-cnn: Towards real-time object detection with region proposal networks. *Advances in neural information processing systems*, 28:91–99, 2015.

[40] Kaiming He, Georgia Gkioxari, Piotr Dollár, and Ross Girshick. Mask r-cnn. In *Proceedings of the IEEE international conference on computer vision*, pages 2961–2969, 2017.